Article

Solubilization of Parabens in Aqueous Pluronic Solutions: Investigating the Micellar Growth and Interaction as a Function of Paraben Composition

M. Khimani,[†] R. Ganguly,*,[‡] V. K. Aswal,[§] S. Nath,[∥] and P. Bahadur[†]

[†]Department of Chemistry, Veer Narmad South Gujarat University, Surat-395007, India
[‡]Chemistry Division, Bhabha Atomic Research Center, Mumbai-400085, India
[§]Solid State Physics Division, Bhabha Atomic Research Center, Mumbai-400085, India
[∥]Radiation and Photochemistry Division, Bhabha Atomic Research Center, Mumbai-400085, India

ABSTRACT: The influence of methyl paraben (MP) and butyl paraben (BP) on the aggregation characteristics of Pluronics in an aqueous medium has been investigated by DLS, SANS, viscometry, and fluorescence measurement techniques. Parabens are extensively used as preservatives in cosmetic, pharmaceutical, and food products. In this paper, we show that their influence on the restructuring and growth of Pluronics micelles vary quite significantly with their aqueous solubility and with the composition of Pluronics. In the case of P105 and P104, MP reduces the sphere-to-rod transition temperature down to room temperature, but BP with significantly less aqueous solubility than MP suppresses such micellar transition and leads to the formation of micellar clusters due to the onset of intermicellar attractive interaction. In the case of more hydrophobic Pluronic P103, on the other hand, both MP and BP are able to induce rapid room temperature sphere-to-rod micellar growth, which is not observed in the presence of water structure making salts like NaCl and Na_3PO_4. These observations have been attributed to modulation of growth and restructuring processes of the Pluronic micelles arising due to different locations of parabens within the micellar corona as determined by their aqueous solubility and the hydrophobicity of the Pluronics.

INTRODUCTION

The commercial PEO-PPO-PEO triblock copolymers, with trademark Pluronics, have attracted the attention of researchers for the last few decades because of their rich phase behavior[1–11] and numerous industrial and biomedical applications.[12–24] In aqueous medium, these copolymers show a strong temperature dependence in their self-assembly characteristics due to the differential solubility characteristics of their constituent blocks.[8] At low temperature, both the PEO end blocks and the PPO middle block are soluble in water and the copolymer remains as molecularly dissolved. At critical micellar temperature (CMT), copolymer molecules assemble through a close association process and form core–shell micelles comprising hydrophobic PPO blocks as core and heavily hydrated hydrophilic PEO blocks as shell (corona).[9–11] Progressive dehydration of these micelles with increase in temperature leads to an increase in aggregation number and core size of micelles.[9,25,26] Such micellar restructuring processes often lead to a sphere-to-rod micellar shape change when the size of the core becomes equal to the length of the stretched PPO chain.[27] Some of these Pluronics, on the other hand, show critical behavior due to the onset of intermicellar attractive interaction and consequent formation of large micellar clusters on approaching the cloud point (CP) of their aqueous solutions.[28–31]

The aggregation characteristics of Pluronics in water are modified quite significantly in the presence of additives that have a strong influence on their solubilization characteristics.[31–45] Substances that increase the hydrophobic character of these copolymers favor micelle formation and growth by reducing the critical micellar concentration (CMC), CMT, and the sphere-to-rod transition temperature of their aqueous solutions. The substances that increase their hydrophilic character, on the other hand, show exactly opposite effects that lead to the destabilization of micelles. Parabens are slightly water-soluble hydrotropes that find widespread uses as preservatives in personal care, pharmaceuticals, and food products because of their bactericidal and fungicidal properties.[46–70] It has been observed that they work only in the aqueous medium and their effectiveness decreases in the presence of surfactants because of their entrapment in the micelles.[71–80] Their effect on aqueous Pluronic systems, however, is important in view of its possible application as preservatives in Pluronic based formulations. It has been shown that parabens increase the hydrophobicity of the Pluronic molecules by interacting with them and consequently decrease

the CMC and gelation temperature of the aqueous Pluronic solutions.[76−79] The effect of parabens on the growth and interaction of the Pluronic micelles which can have significant influence on the rheological behavior of the Pluronic based formulations[24] are, however, not understood. In view of this, we have carried out detailed studies on the effect of solubilization of two parabens, namely, methyl paraben and butyl paraben, on the aggregation characteristics of three Pluronics with varying hydrophobicity, namely, P105, P104, and P103. The results show that, though these two parabens in general dehydrate micelles of all three Pluronics, the aqueous solubility and hydrophobicity of the pluronic play important roles in determining the micellar restructuring process and subsequently in modulating the micellar growth and interaction.

■ EXPERIMENTAL SECTION

Materials and Sample Preparation. The Pluronics P103, P104, and P105 were procured from BASF Corp., Parsippany, NJ, and were used as received. Methyl and butyl parabens (Scheme 1) were synthesized in our laboratory. The copolymer

Scheme 1
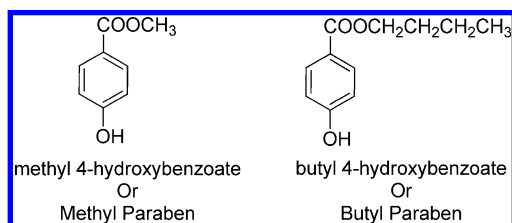
solutions were prepared by weighing required amounts of water and copolymer and keeping them in a refrigerator overnight in tightly closed glass vials. The concentration of the copolymer solutions used (5%) is well above the CMCs of three pluronics at 30 °C, which are 0.01, 0.04, and 0.025% for P103, P104, and P105, respectively.[8] At this concentration, the copolymer solutions do not form any liquid crystalline phase but show sphere-to-rod shape transition on approaching their cloud points.

Methods. *Dynamic Light Scattering (DLS).* DLS measurements were performed using a Malvern 4800 Autosizer employing a 7132 digital correlator. The light source was a He−Ne laser operated at 633 nm with a maximum output power of 15 mW. The average decay rate was obtained by analyzing the electric field autocorrelation function, $g^1(\tau)$, vs time data using a modified cumulants method or a double exponential equation.[81] This modified cumulant method overcomes the limitations of cumulants analysis to fit the autocorrelation function data of samples with large polydispersity.[82] The apparent equivalent hydrodynamic radii of the micelles were calculated using the Stokes−Einstein equation. Measurements were made at 90° scattering angle.

Viscometry. The absolute viscosities of the solutions were measured in a temperature controlled water bath by using size 50, size 150, and size 300 calibrated cannon Ubbelohde viscometers, with viscometer constants of 0.004065, 0.03925, and 0.2775 centi-stokes/s, respectively.[83] The measured flow times of the solutions in seconds were multiplied by the viscometer constant to get the kinematic viscosity of the solutions in centi-stokes. The spread in flow times was found to remain within ±5 s. These kinematic viscosities were then multiplied by the density of water (taken as 1 g/cm³) to obtain

the viscosity of the solutions in centi-poise. The relative viscosities of the solutions were then calculated by dividing the obtained viscosity values by the viscosity of water at room temperature.

Small Angle Neutron Scattering (SANS). SANS measurements were carried out on the samples prepared in D_2O at the SANS facility at DHRUVA reactor, Trombay. The mean incident wavelength was 5.2 Å with $\Delta\lambda/\lambda = 15\%$. The scattering intensity was measured in the scattering vector (q) range of 0.017−0.3 Å^{-1}. The measured SANS data were corrected for the background, the empty cell contributions, and the transmission and were placed on an absolute scale using standard protocols. Correction due to the instrumental smearing was taken into account throughout the data analysis.[84]

Steady State Fluorescence. Steady-state fluorescence spectra were recorded using a Hitachi (Tokyo, Japan) model F-4010 spectrofluorometer. The recorded spectra were corrected for wavelength dependent instrument responses by measuring the spectrum of quinine sulfate and comparing it with the reported standard spectrum.[85] All the emission spectra were recorded at 30 °C. The fluorescence probe used for the present study is Coumarin-153 (C153). The Pluronic concentration used was such that the probability of having more than one C153 molecule in a single micelle was very low.

Dipole Moment Calculation. The quantum chemical calculations of the dipole moment of MP and BP were carried out by using a Gaussian 03 software package. The ground-state geometry was optimized by using the density functional theory (DFT). Becke's three-parameter hybrid exchange function with the Lee−Yang−Parr gradient corrected correlated functional (B3LYP) was used in conjunction with the 6-311++ (d,p) basis set. The effect of solvent dielectric on the ground-state geometry was modeled by performing self-consistent reaction field (SCRF) calculations using the polarizable continuum model (PCM).

■ RESULTS AND DISCUSSION

The Effect of Methyl Paraben. The aqueous solutions of Pluronics P103, P104, and P105 are known to exhibit sphere-to-rod micellar shape transition upon micellar dehydration either with increase in temperature or in the presence of different water structure making additives.[86−89] Such structural transitions are rapid in P104 and P105 solutions but are slow and time dependent in P103 solutions because of slow restructuring of the P103 micelles.[89] To study how the parabens influence the aggregation characteristics of these Pluronics, we first studied their effect on the phase separation characteristics (cloud point) of the copolymer solutions, as represented in Figure 1. Figure 1a shows that CP of pure copolymer solutions decreases from P105 (above 100 °C) to P104 but then increases significantly to P103. This is against the expectation, since the hydrophobic character of these copolymers increases in the order P105 < P104 < P103. The reason for this is that the restructuring process of the micelles slows down with an increase in the hydrophobicity of the copolymers,[90,91] which retards the phase separation process so that it occurs at higher temperature than the actual CP.[92] The copolymer P123 ($EO_{20}PO_{70}EO_{20}$), whose hydrophobicity is comparable to that of P103, also shows a similar behavior in the aqueous medium because of slow micellar restructuring.[89,92]

Figure 1a also shows the effect of MP on the CP of the three copolymer solutions. A monotonous decrease in CP with an increase in MP concentration in the case of all three
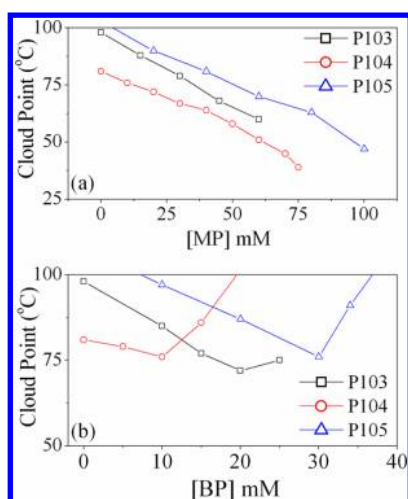
Figure 1. Cloud point (CP) of the 5% pluronic solutions as a function of (a) MP and (b) BP concentration.

copolymers suggests that the presence of MP leads to dehydration of the copolymer micelles. As shown in Figure 2,
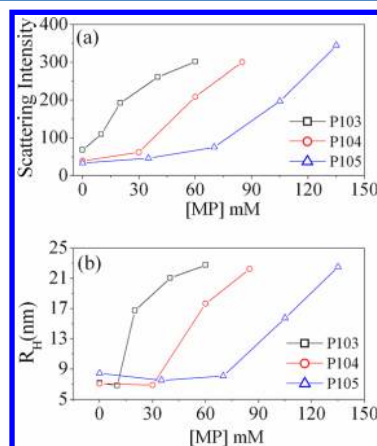

Figure 2. (a) Light scattering intensity and (b) hydrodynamic size of the micelles in 5% pluronic solutions as a function of MP concentration at 30 °C.

this is accompanied by a large increase in light scattering intensity and a simultaneous micellar growth at the room temperature. Figure 3 shows that the observed micellar growth results in a large increase in viscosity of the copolymer solution at 30 °C. Observations of a simultaneous micellar growth and
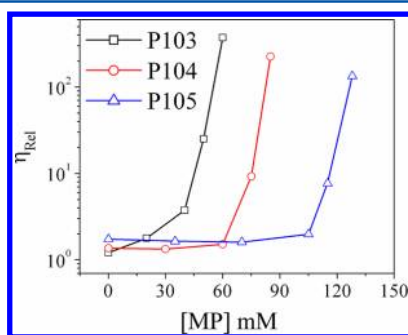
Figure 3. The relative viscosity of 5% pluronic solutions as a function of MP concentration at 30 °C.

enhancement in viscosity suggest that the micelles of all three copolymers undergo sphere-to-rod shape transition in the presence of MP. SANS studies on P103 solutions, which are shown in Figure 4, support this conjecture. It shows that the
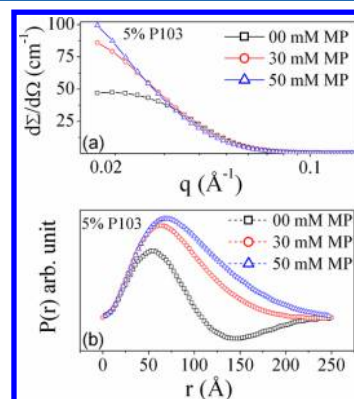

Figure 4. (a) SANS patterns of 5% P103 solutions at 30 °C as a function of MP concentration. (b) The corresponding pair distance distribution function $[P(r)]$ plots.

scattering intensity increases monotonously with an increase in MP concentration (Figure 4a), which can be attributed either to sphere-to-rod micellar growth or to micellar cluster formation resulting due to the presence of attractive inter-micellar interaction. To verify the state of the micellar aggregates, we calculated the pair distance distribution functions $[p(r)]$ from the SANS plots using the program GNOM developed by Svergun and Semenyuk.[93,94] As shown in Figure 4b, the $p(r)$ plot becomes more and more asymmetric with an increase in MP concentration. This suggests that P103 micelles undergo sphere-to-rod micellar shape transition as a result of micellar growth. These results thus show that solubilization of MP not only reduces the sphere-to-rod micellar shape transition temperature in P105 and P104 solutions down to room temperature but also induces a rapid room temperature growth of P103 micelles, which is not observed in the presence of water structure making salts like NaCl and Na_3PO_4.[89]

The Effect of Butyl Paraben. We will now discuss the evolution of the properties of the copolymer solutions upon solubilization of BP, which has about an order of magnitude lower aqueous solubility than that of MP. As shown in Figure 1b, for all three copolymer solutions, BP reduces the cloud point up to a certain concentration and increases it quite sharply beyond it. This suggests that, like MP, BP also increases the hydrophobicity of the Pluronic molecules, but it has an additional effect of slowing down the restructuring process of the copolymer micelles at a higher level of solubilization. This results in the occurrence of phase separation at a temperature much higher than the actual CP, similar to what is observed in the aqueous solutions of P103 and P123.[92] The observed effect on CP is also accompanied by disappearance of the sphere-to-rod transition of the copolymer micelles as reflected in the absence of any viscosity enhancement on approaching the CP (not shown).

The influence of solubilization of BP on the micellar aggregation characteristics and the viscosity of the copolymer solutions at 30 °C are presented in Figures 5–8. Figure 5 shows that in the case of all three copolymer solutions the scattering intensity increases with BP concentration, which suggests that
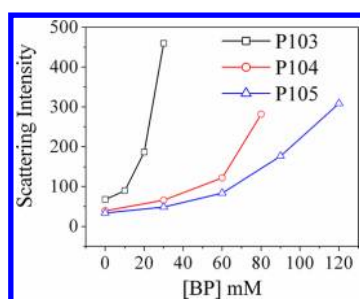
Figure 5. Light scattering intensity in 5% pluronic solutions as a function of BP concentration at 30 °C.

solubilization of BP improves the aggregation characteristics of the copolymers. For P103, the observed increase in the scattering intensity is accompanied by a micellar growth and consequent increase in the viscosity of the copolymer solutions at 30 °C (Figure 6). This suggests that, like in the case of MP, BP also induces a room temperature sphere-to-rod growth of the P103 micelles.
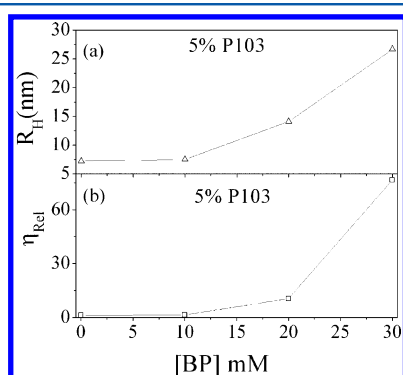

Figure 6. (a) Hydrodynamic size of the micelles in 5% P103 solution and (b) relative viscosity of 5% P103 solution as a function of BP concentration at 30 °C.

The situation is very different in the case of P104 and P105, both of which do not show any micellar growth and any increase in solution viscosity upon solubilization of BP. CONTIN analyses[95] of the correlation function data carried out on the basis of inverse Laplace transformation

$$g^1(t) = \int_{-\alpha}^{\alpha} \tau A(\tau) e^{-t/\tau} \, d(\ln \tau)$$

suggest that the observed increase in scattering intensity arises due to the formation of micellar clusters. This is shown in Figures 7 and 8, which show a comparison of the correlation function and relaxation time distribution plots of the P104 and P105 solutions in the presence and absence of BP, respectively. These plots clearly show that addition of BP leads to formation of micellar clusters without any detectable growth of the micelles. SANS studies shown in Figure 9 also support this conjecture, as the observed increase in the scattering intensity (Figure 9a) upon addition of BP in 5% P105 solution does not lead to any increase in anisotropy of the aggregates present (Figure 9b). The observed suppression of the sphere-to-rod shape transition of P104 and P105 micelles thus supports the conjecture made from the results of the CP measurements that solubilization of BP slows down the restructuring process of the P104 and P105 micelles. These two copolymers, however, did show a difference in their growth behavior when the time
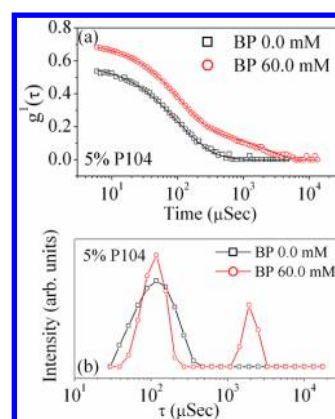
Figure 7. (a) Correlation function diagram of 5% P104 solution recorded at 30 °C and at 90° scattering angle as a function BP concentration. The solid lines represent a fit to the data. (b) The corresponding relaxation time distribution plots obtained from CONTIN analysis of the correlation function data.
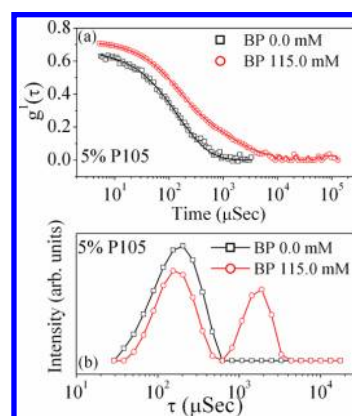
Figure 8. (a) Correlation function diagram of 5% P105 solution recorded at 30 °C and at 90° scattering angle as a function of BP concentration. The solid lines represent a fit to the data. (b) The corresponding relaxation time distribution plots obtained from CONTIN analysis of the correlation function data.
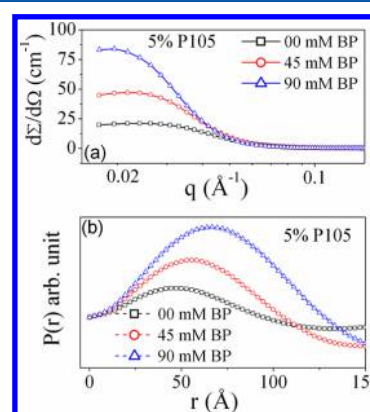
Figure 9. (a) SANS patterns of 5% P105 solutions at 30 °C as a function of BP concentration. (b) The corresponding pair distance distribution function $[P(r)]$ plots.

dependence of their aggregation characteristics was studied by DLS and viscosity measurements. It was observed that, whereas P104 solution containing 60 mM BP shows an increase in viscosity and a corresponding micellar growth with increase in time when the solution is kept at ambient conditions (Figure

10), the P105 solutions do not show any such effect. The growth in P104 micelles with time is reflected in shift in the

Figure 10. (a) Correlation function diagram of 5% P104 solution with 60 mM BP recorded at 30 °C and at 90° scattering angle as a function of time. The solid lines represent a fit to the data. (b) The corresponding relaxation time distribution plots obta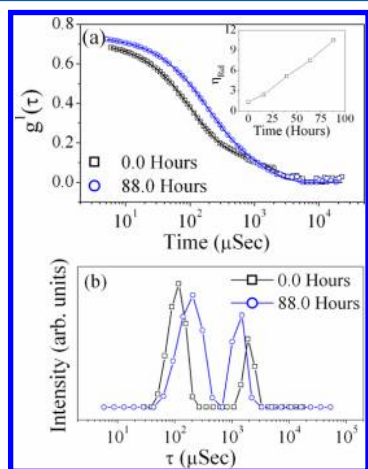ined from CONTIN analysis of the correlation function data. The inset shows the relative viscosity of the solution as a function of time when kept at ambient conditions.

correlation function data and the relaxation time distribution of the micelles to higher time scale. An increase in viscosity of the solution with time suggests that the micellar growth is associated with a sphere-to-rod shape transition. These observations suggest that BP induced slowing down of the micellar restructuring process becomes increasingly effective as the hydrophilic character of the Pluronics increases. Absence of such effects in the case of MP suggests that the location of the two parabens within the micelles could be different due to the difference in their aqueous solubility. To shed further light on this, we will now discuss the effect of solubilization of MP and BP in P105 solutions on fluorescence emission spectra of C153.

Steady State Fluorescence Studies. In order to understand the difference in the behavior of two parabens, we measured the fluorescence emission spectra of C153 in 5% P105 solutions in the presence of 100 mM MP and BP. The emission maximum of C153 is known to be sensitive to the polarity of its surrounding medium.[95] It undergoes a blue shift with a decrease in the polarity of the medium and a red shift with an increase in the same. Since in the case of Pluronics this probe preferentially resides in the micellar corona region,[96] any change in the polarity of this region can be monitored through its emission maximum. In the present case, the dehydration of P105 micelles upon addition of parabens is expected to lead to a blue shift of the emission maximum.[96] Contrary to that expectation, Figure 11 shows that the emission maximum of C153 is red-shifted upon addition of 100 mM MP and BP, the extent of shift being very similar in the two cases. A decrease in the polarity of the micellar corona region due to the dehydration of the copolymer molecules is thus more than compensated by the presence of the two parabens, which suggests that paraben molecules preferentially occupy the corona region of micelles. Since the dipole moments of both the parabens (2.48 for MP and 2.06 for BP as calculated by us) are higher than that of water (1.85), their presence in the corona region as a substitute of water can lead to the observed
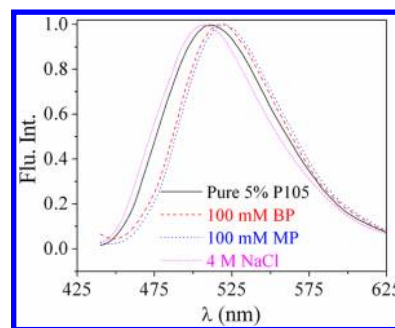
Figure 11. Intensity normalized fluorescence spectra of C153 in 5% P105 solutions recorded at 30 °C.

increase in polarity of the micellar corona. Figure 11 also shows the emission spectra for P105 solution in the presence of 4 M NaCl. This salt is known to cause dehydration of Pluronic micelles due to the water structure making abilities of its constituent ions. It can be seen from Figure 11 that, as expected, the emission maximum gets blue-shifted in the presence of 4 M NaCl. The opposite behavior of these two cases, in spite of a very similar effect on CP, thus again suggests that both of the parabens preferentially occupy the micellar corona region. The difference in the behavior of two parabens thus could arise due to the difference in their locations in the micellar corona. As the copolymer becomes more and more hydrophilic, the less soluble BP may prefer to stay closer to the core−corona interface as compared to MP and thus could influence the micellar restructuring process to a different degree. It has been suggested in the literature that it is the dehydration of the micellar corona which controls the kinetics of the sphere-to-rod shape transition in Pluronic micelles.[89,97] The location of BP close to the micellar core and consequently a reduced degree of dehydration of the micellar corona could thus be the reason for the slow restructuring and subsequently retarded sphere-to-rod growth of the P104 and P105 micelles in the presence of BP.

Bilayered Structure Formation. Aqueous solutions of Pluronics exhibit a sphere-to-rod micellar transition near cloud point.[27] In the present case, however, though P103 and P104 solutions containing BP show formation of worm-like micelles at room temperature, the phase separation in them occurs at much higher temperature (Figure 1). In order to understand the evolution of the properties of these two Pluronic solutions on approaching the phase separation temperature, we have carried out DLS, SANS, and viscosity studies on 5% P104 solution with 60 mM BP as a function of temperature. This solution shows time dependent sphere-to-rod micellar growth and as depicted in Figure 10, undergoes about an order of magnitude increase in viscosity after 88 h of equilibration. Figure 12a shows that the viscosity of this solution decreases sharply with an increase in temperature, which suggests that the rod-like micelles formed upon equilibration break down upon heating. Quite interestingly, as shown in the figure, the observed decrease in viscosity of the solution is accompanied by an increase in light scattering intensity and a simultaneous increase in the size of the aggregates (Figure 12b). The nature of the variation of the correlation function data also changes from biexponential to single exponential, which arises due to diminished role of entangled worm-like micelles and large micellar clusters as scattering species upon warming. To get an idea about the structure of the aggregates formed in the sample with an increase in temperature, we carried out SANS studies
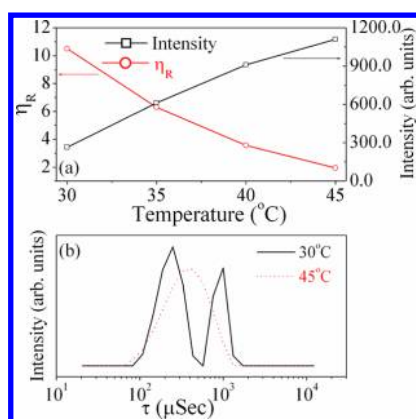
Figure 12. (a) Light scattering intensity and relative viscosity as a function of temperature for 5% P104 solutions with 60 mM BP after 88 h of equilibration. (b) Relaxation time distribution plots obtained from CONTIN analysis of the correlation function data for the same sample at 30 °C and 45 °C.

on 5% P104 solution with 60 mM BP at 30 and 50 °C after equilibrating it at room temperature for 48 h (Figure 13). The
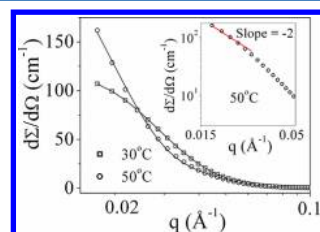
Figure 13. SANS patterns of 5% P104 solutions with 60 mM BP after 88 h of equilibration at 30 and 50 °C. The solid lines represent fits to the data. The inset shows the slope of −2 (q^{-2} variation of scattering cross section) of the data at 50 °C in the low q region on log−log scale.

change in the structure of the aggregates as the temperature increases from 30 to 50 °C is evident from the change in the nature of the SANS plot. An increase in slope in the low q zone and shift of the plot to lower q region are manifestations of the formation of a large bilayered structure.[98,100] Analysis of the data by the SASFIT program[101] shows that the observed change in the SANS plot with increase in temperature is indeed associated with a change in the structure of the aggregates present in the solution. The plot at 30 °C can be fit based on a rod-like structure having 4.1 nm radius and 14.6 nm length. On the other hand, the plot at 50 °C can be best fit based on a disk-like (bilayered) structure with a semiminor axis of 3.7 nm and semimajor axis of 13.6 nm. The q^{-2} dependence of the scattering intensity in the low q region (Figure 13, inset) is also suggestive of the presence of disk-like structure.[100] Bilayered structures are reported to form in the aqueous solutions of hydrophobic Pluronics like P123, L121, etc.[102−104] Our results show that the formation of such structures can be extended to Pluronics with less hydrophobicity. The results also suggest that the kinetics of the micellar restructuring process plays an important role in the formation of bilayered structure in these systems. As the micellar restructuring process and the phase separation characteristics are retarded in P104 solution in the presence of BP, the rod-like micelles are converted to bilayered structure as the critical packing parameter of Pluronic assemblies decreases due to dehydration of the copolymer

molecules with increase in temperature. The observed transformation of the copolymer aggregates has been found to be reversible, and the copolymer solution regains its viscosity upon cooling to room temperature.

■ CONCLUSION

In view of the potential applicability of parabens as preservatives in Pluronic formulations, we have studied the influence of solubilization of methyl and butyl paraben in the aqueous solutions of three Pluronics with varying hydrophobicity. The studies show that solubilization of both of the parabens increases the hydrophobicity of the Pluronics micelles and leads to a decrease in CP of the Pluronic solutions. The influence of these parabens on the micellar growth and interaction, however, depends significantly on their aqueous solubility and the hydrophobicity of Pluronics. Both of the parabens induce a rapid sphere-to-rod micellar growth of P103 micelles at room temperature. The situation is different in the case of more hydrophilic copolymers P104 and P105, where methyl paraben brings down the sphere-to-rod transition temperature and induces a room temperature sphere-to-rod micellar growth. Butyl paraben, with 1 order of magnitude lower aqueous solubility than methyl paraben, on the other hand, suppresses such micellar growth and leads to the formation of micellar clusters due to the onset of inter-micellar attractive interaction. This has been explained on the basis of slowing down of the micellar restructuring process upon solubilization of butyl paraben. Quite interestingly, such BP induced slowing down of the micellar restructuring process leads to the formation of large bilayered structure in P104 solution on approaching the phase separation temperature. The observed difference in the behavior of MP and BP has been suggested to arise due to the difference in their location within the micelles as determined by their solubility. The observation of such systematic modulation of the hydrotrope induced micellar restructuring and growth processes determined by their locations within the micelles is first of its kind in aqueous Pluronic systems.

■ AUTHOR INFORMATION

Corresponding Author
*E-mail: rajibg@barc.gov.in, rajugang@yahoo.co.in. Phone: +91-22-25590286. Fax: +91-22-25505151.

Notes
The authors declare no competing financial interest.

■ REFERENCES

(1) Chu, B. *Langmuir* **1995**, *11*, 414−421.
(2) Wanka, G.; Hoffmann, H.; Ulbricht, W. *Macromolecules* **1994**, *27*, 4145−4159.
(3) Hurter, P. N.; Hatton, T. A. *Langmuir* **1992**, *8*, 1291−1299.
(4) Zhang, K.; Khan, A. *Macromolecules* **1995**, *28*, 3807−3812.
(5) Hvidt, S.; Joergensen, E. B.; Brown, W.; Schillen, K. *J. Phys. Chem.* **1994**, *98*, 12320−12328.
(6) Mortensen, K.; Brown, W.; Nordén, B. *Phys. Rev. Lett.* **1992**, *68*, 2340−2343.
(7) Malmsten, M.; Lindman, B. *Macromolecules* **1993**, *26*, 1282−1286.
(8) Alexandridis, P.; Holzwarth, J. F.; Hatton, T. A. *Macromolecules* **1994**, *27*, 2414−2425.
(9) Wanka, G.; Hoffmann, H.; Ulbricht, W. *Colloid Polym. Sci.* **1990**, *268*, 101−117.
(10) Glatter, O.; Scherf, G.; Schillen, K.; Brown, W. *Macromolecules* **1994**, *27*, 6046−6054.

(11) Brown, W.; Schillen, K.; Almgren, M.; Hvidt, S.; Bahadur, P. *J. Phys. Chem.* **1991**, *95*, 1850−1858.

(12) Schmolka, I. R. *J. Am. Oil Chem. Soc.* **1977**, *54*, 110−116.

(13) Pandit, N. K.; Wang, D. *Int. J. Pharm.* **1998**, *167*, 183−189.

(14) Husseini, G. A.; Abdel-Jabbar, N. M.; Mjalli, F. S.; Pitt, W. G.; Al-Mousa, A. *J. Franklin Inst.* **2011**, *348*, 1276−1284.

(15) Husseini, G. A.; Abdel-Jabbar, N. M.; Mjalli, F. S.; Pitt, W. G. *Technol. Cancer Res. Treat.* **2007**, *6*, 49−56.

(16) Husseini, G. A.; Diaz de la Rosa, M. A.; AlAqqad, E. O.; Al Mamary, S.; Kadimati, Y.; Al Baik, A.; Pitt, W. G. *J. Franklin Inst.* **2011**, *348*, 125−133.

(17) Kulthe, S. S.; Inamdar, N. N.; Choudhari, Y. M.; Shirolikar, S. M.; Borde, L. C.; Mourya, V. K. *Colloids Surf., B* **2011**, *88*, 691−696.

(18) Choi, W. I.; Lee, J. H.; Kim, J. Y.; Kim, J. C.; Kim, Y. H.; Tae, G. *J. Controlled Release* **2012**, *157*, 272−278.

(19) Zhang, W.; Shi, Y.; Chen, Y.; Ye, J.; Sha, X.; Fang, X. *Biomaterials* **2011**, *32*, 2894−2906.

(20) Zhang, W.; Shi, Y.; Chen, Y.; Yu, S.; Hao, J.; Luo, J.; Sha, X.; Fang, X. *Eur. J. Pharm. Biopharm.* **2010**, *75*, 341−353.

(21) Witt, K. A.; Huber, J. D.; Egleton, R. D.; Davis, T. P. *J. Pharmacol. Exp. Ther.* **2002**, *303*, 760−767.

(22) Lai, T. C.; Kataoka, K.; Kwon, G. S. *Biomaterials* **2011**, *32*, 4594−4603.

(23) Batrakova, E. V.; Li, S.; Li, Y.; Alakhov, V. Y.; Elmquist, W. F.; Kabanov, A. V. *J. Controlled Release* **2004**, *100*, 389−397.

(24) Parekh, P.; Ganguly, R.; Aswal, V. K.; Bahadur, P. *Soft Matter* **2012**, *8*, 5864−5872.

(25) Al-Saden, A.; Whateley, T.; Florence, A. *J. Colloid Interface Sci.* **1982**, *90*, 303−309.

(26) Zhou, Z.; Chu, B. *J. Colloid Interface Sci.* **1988**, *126*, 171−180.

(27) Mortensen, K.; Pedersen, J. S. *Macromolecules* **1993**, *26*, 805−812.

(28) Chen, W. R.; Mallamace, F.; Glinka, C. J.; Fratini, E.; Chen, S. H. *Phys. Rev. E* **2003**, *68*, 041402−041416.

(29) Ganguly, R.; Choudhury, N.; Aswal, V. K.; Hassan, P. A. *J. Phys. Chem. B* **2009**, *113*, 668−675.

(30) Kositza, M. J.; Bohne, C.; Alexandridis, P.; Hatton, T. A.; Holzwarth, J. F. *Macromolecules* **1999**, *32*, 5539−5551.

(31) Ganguly, R.; Kuperkar, K.; Parekh, P.; Aswal, V. K.; Bahadur, P. *J. Colloid Interface Sci.* **2012**, *378*, 118−124.

(32) Alexandridis, P.; Holzwarth, J. F. *Langmuir* **1997**, *13*, 6074−6082.

(33) Ganguly, R.; Aswal, V. K.; Hassan, P. A.; Gopalakrishnan, I. K.; Yakhmi, J. V. *J. Phys. Chem. B* **2005**, *109*, 5653−5658.

(34) Armstrong, J.; Chowdhry, B.; Mitchell, J.; Beezer, A.; Leharne, S. *J. Phys. Chem.* **1996**, *100*, 1738−1745.

(35) Ivanova, R.; Lindman, B.; Alexandridis, P. *Adv. Colloid Interface Sci.* **2001**, *89*, 351−382.

(36) Holmqvist, P.; Alexandridis, P.; Lindman, B. *Langmuir* **1997**, *13*, 2471−2479.

(37) Holmqvist, P.; Alexandridis, P.; Lindman, B. *J. Phys. Chem. B* **1998**, *102*, 1149−1158.

(38) Holmqvist, P.; Alexandridis, P.; Lindman, B. *Macromolecules* **1997**, *30*, 6788−6797.

(39) Guo, L.; Colby, R. H.; Thiyagarajan, P. *Phys. B* **2006**, *385*, 685−687.

(40) Su, Y.-l.; Wei, X.-f.; Liu, H.-z. *Langmuir* **2003**, *19*, 2995−3000.

(41) Caragheorgheopol, A.; Caldararu, H.; Dragutan, I.; Joela, H.; Brown, W. *Langmuir* **1997**, *13*, 6912−6921.

(42) Ma, J.-H.; Wang, Y.; Guo, C.; Liu, H.; Tang, Y.; Bahadur, P. *J. Phys. Chem. B* **2007**, *111*, 11140−11148.

(43) Mata, J. P.; Majhi, P. R.; Kubota, O.; Khanal, A.; Nakashima, K.; Bahadur, P. *J. Colloid Interface Sci.* **2008**, *320*, 275−282.

(44) Heerema, L.; Cakali, D.; Roelands, M.; Goetheer, E.; Verdoes, D.; Keurentjes, J. *Sep. Purif. Technol.* **2010**, *73*, 319−326.

(45) Ganguly, R.; Aswal, V. K.; Hassan, P. A.; Gopalakrishnan, I. K.; Kulshreshtha, S. K. *J. Phys. Chem. B* **2006**, *110*, 9843−9849.

(46) Wallhauser, K. H., Rieger, M. M., Ed. *Surfactants in Cosmetics*; Surfactant Science Series; Marcel Dekker: New York, 1985; Vol. 16, p 211.

(47) Soni, M. G.; Burdock, G. A.; Taylor, S. L.; Greenberg, N. A. *Food Chem. Toxicol.* **2001**, *39*, 513−532.

(48) Soni, M. G.; Taylor, S.; Greenberg, N.; Burdock, G. *Food Chem. Toxicol.* **2002**, *40*, 1335−1373.

(49) Berke, P. A.; Steinberg, D. C.; Rosen, W. E. *Cosmet. Toiletries* **1982**, *97*, 89−93.

(50) Elder, R. L. *J. Am. Coll. Toxicol.* **1984**, *3*, 147−209.

(51) Perlovich, G. L.; Rodionov, S. V.; Bauer-Brandl, A. *Eur. J. Pharm. Sci.* **2005**, *24*, 25−33.

(52) Neidig, C. P.; Burrell, H. *Drug Cosmet. Ind.* **1944**, *54*, 408−410.

(53) Neidig, C. P.; Burrell, H. *Drug Cosmet. Ind.* **1944**, *54*, 481−489.

(54) Jackson, E. M. *Cutaneous Ocul. Toxicol.* **1992**, *11*, 173−184.

(55) Maddox, D. *Cosmet. Toiletries* **1982**, *97*, 85−88.

(56) Weber, R. W. *Ann. Allergy* **1993**, *70*, 183−190.

(57) Rastogi, S. C.; Schouten, A.; Kruijf, N. D.; Weijland, J. W. *Contact Dermatitis* **1995**, *32*, 28−30.

(58) Daniel, J. W. *Xenobiotica* **1986**, *16*, 1073−1078.

(59) Sabalitschka, T. *Arch. Pharm.* **1930**, *268*, 653−673.

(60) Hassler, W. H. *Am. Prof. Pharm.* **1954**, *20*, 527.

(61) Boehm, E. E.; Maddox, D. N. *Manuf. Chem. Aerosol News* **1972**, *43*, 21−23.

(62) Orth, D. S. *Int. J. Dermatol.* **1980**, *19*, 504−505.

(63) Robach, M. C. *Food Technol* **1980**, *34*, 81−84.

(64) Dziezak, J. D. *Food Technol.* **1986**, *40*, 104−111.

(65) Liao, X.; Raghavan, G. S. V.; Yaylayan, V. A. *Tetrahedron Lett.* **2002**, *43*, 45−48.

(66) Wille, S.; Mokrushina, L.; Smirnova, I.; Arlt, W. *Chem. Eng. Technol.* **2010**, *33*, 2095−2101.

(67) Rocca, S.; Garcia-Celma, M. J.; Caldero, G.; Pons, R.; Solans, C.; Stebe, M. J. *Langmuir* **1998**, *14*, 6840−6845.

(68) Watrobska-Swietlikowska, D.; Sznitowska, M. *Int. J. Pharm.* **2006**, *312*, 174−178.

(69) Sznitowska, M.; Janicki, S.; Dabrowska, E. A.; Gajewska, M. *Eur. J. Pharm. Sci.* **2002**, *15*, 489−495.

(70) Yamaguchi, M.; Asaka, Y.; Tanaka, M.; Mitsui, T.; Ohta, S. *J. Soc. Cosmet. Chem.* **1982**, *33*, 297−307.

(71) Fukahori, M.; Takatsuji, Y.; Akatsu, S.; Sato, H.; Yotsuyanagi, T. *Biocontrol Sci.* **1998**, *3*, 23−29.

(72) Goto, A.; Nihei, M.; Endo, F. *J. Phys. Chem.* **1980**, *84*, 2268−2272.

(73) Fukahori, M.; Takatsuji, Y.; Takahashi, H.; Sato, H.; Yotsuyanagi, T. *Chem. Pharm. Bull.* **1996**, *44*, 1068−1073.

(74) Fukahori, M.; Takatsuji, Y.; Seki, M.; Takahashi, H.; Sato, H.; Yotsuyanagi, T. *Chem. Pharm. Bull.* **1996**, *44*, 577−581.

(75) Fukahori, M.; Akatsu, S.; Sato, H.; Yotsuyanagi, T. *Chem. Pharm. Bull.* **1996**, *44*, 1567−1570.

(76) Sharma, P. K.; Reilly, M. J.; Bhatia, S. K.; Sakhitab, N.; Archambault, J. D.; Bhatia, S. R. *Colloids Surf., B* **2008**, *63*, 229−235.

(77) Sharma, P. K.; Reilly, M. J.; Jones, D. N.; Robinson, P. M.; Bhatia, S. R. *Colloids Surf., B* **2008**, *61*, 53−60.

(78) Meznarich, N. A. K.; Love, B. J. *Macromolecules* **2011**, *44*, 3548−3555.

(79) Meznarich, N. A. K.; Juggernauth, K. A.; Batzli, K. M.; Love, B. J. *Macromolecules* **2011**, *44*, 7792−7798.

(80) Pandit, N.; Trygstad, T.; Croy, S.; Bohorquez, M.; Koch, C. *J. Colloid Interface Sci.* **2000**, *222*, 213−220.

(81) Hassan, P. A.; Kulshreshtha, S. K. *J. Colloid Interface Sci.* **2006**, *300*, 744−748.

(82) Koppel, D. E. *J. Chem. Phys.* **1972**, *57*, 4814−4820.

(83) ASTM Standard D 445-04 and D 446-04 2004 and the references within.

(84) Aswal, V. K.; Goyal, P. S. *Curr. Sci.* **2000**, *79*, 947−953.

(85) Velapoldi, R. A.; Mielenz, K. D. *A fluorescence standard reference material: quinine sulfate dihydrate*; National Bureau of Standards: Washington, DC, 1980; Special Publication Number *260*.

(86) Álvarez-Ramírez, J. G.; Fernández, V. V. A.; Macías, E. R.; Rharbi, Y.; Taboada, P.; Gámez-Corrales, R.; Puig, J. E.; Soltero, J. F. A. *J. Colloid Interface Sci.* **2009**, *333*, 655−662.

(87) Foster, B.; Cosgrove, T.; Hammouda, B. *Langmuir* **2009**, *25*, 6760−6766.

(88) Guo, L.; Colby, R. H.; Lin, M. Y.; Dado, G. P. *J. Rheol.* **2001**, *45*, 1223−1243.

(89) Kadam, Y.; Ganguly, R.; Kumbhakar, M.; Aswal, V. K.; Hassan, P. A.; Bahadur, P. *J. Phys. Chem. B* **2009**, *113*, 16296−16302.

(90) Waton, G.; Michels, B.; Zana, R. *J. Colloid Interface Sci.* **1999**, *212*, 593−596.

(91) Kositza, M. J.; Bohne, C.; Alexandridis, P.; Hatton, T. A.; Holzwarth, J. F. *Langmuir* **1999**, *15*, 322−325.

(92) Ganguly, R.; Kumbhakar, M.; Aswal, V. K. *J. Phys. Chem. B* **2009**, *113*, 9441−9446.

(93) Svergun, D.; Semenyuk, A.; Feigin, L. *Acta Crystallogr., Sect. A* **1988**, *44*, 244−250.

(94) Svergun, D. *J. Appl. Crystallogr.* **1991**, *24*, 485−492.

(95) Provencher, S. W. *Comput. Phys. Commun.* **1982**, *27*, 229−242.

(96) Kumbhakar, M. *J. Phys. Chem. B* **2007**, *111*, 14250−14255.

(97) Löf, D.; Niemiec, A.; Schillén, K.; Loh, W.; Olofsson, G. *J. Phys. Chem. B* **2007**, *111*, 5911−5920.

(98) Nieh, M.-P.; Kučerka, N.; Katsaras, J. *Can. J. Phys.* **2010**, *88*, 735−740.

(99) Nieh, M. P.; Dolinar, P.; Kučerka, N.; Kline, S. R.; Debeer-Schmitt, L. M.; Littrell, K. C.; Katsaras, J. *Langmuir* **2011**, *27*, 14308−14316.

(100) Verma, G.; Aswal, V. K.; Fritz-Popovski, G.; Shah, C. P.; Kumar, M.; Hassan, P. A. *J. Colloid Interface Sci.* **2011**, *359*, 163−170.

(101) Kohlbrecher, J.; Bressler, I. *Software package SASFIT for fitting small-angle scattering curves*, 2009; http://kur.web.psi.ch/sans1/SANSSoft/sasfit.html.

(102) Chen, S.; Yang, B.; Guo, C.; Ma, J.-H.; Yang, L.-R.; Liang, X.; Hua, C.; Liu, H.-Z. *J. Phys. Chem. B* **2008**, *112*, 15659−15665.

(103) Sakai, T.; Kurosawa, H.; Okada, T.; Mishima, S. *Colloids Surf., A* **2011**, *389*, 82−89.

(104) Zipfel, J.; Lindner, P.; Tsianou, M.; Alexandridis, P.; Richtering, W. *Langmuir* **1999**, *15*, 2599−2602.